Molecular Pharmacology Fast Forward. Published on December 23, 2019 as DOI: 10.1124/mol.119.117192
This article has not been copyedited and formatted. The final version may differ from this version.

Structural determinants of Kv7.5 potassium channels that confer changes in phosphatidylinositol 4,5-bisphosphate (PIP_2) affinity and signaling sensitivities in smooth muscle cells

Lyubov I. Brueggemann, Leanne L. Cribbs, and Kenneth L. Byron

Loyola University Chicago, Stritch School of Medicine, Department of Molecular Pharmacology & Therapeutics (LIB, KLB) and Department of Cell and Molecular Physiology (LLC), Maywood, IL USA

Molecular Pharmacology Fast Forward. Published on December 23, 2019 as DOI: 10.1124/mol.119.117192
This article has not been copyedited and formatted. The final version may differ from this version.

Running title: PKA and PKC affect PIP_2 binding via N and C termini of Kv7.5

Corresponding author:
Kenneth L. Byron, Ph.D.
Dept. of Molecular Pharmacology & Therapeutics
Loyola University Chicago
2160 S. First Avenue
Maywood, IL 60153, USA
Tel: 708-327-2819
Email: kbyron@luc.edu

Text pages **20**
Tables **0**
Figures **8**
References **34**
Number of words in the:

Abstract	250
Introduction	581
Discussion	2393

Abbreviations:

4αPMA, 4α-phorbol-12-myristate-13-acetate

AVP, arginine vasopressin

cAMP, cyclic adenosine monophosphate

βAR, beta-adrenergic receptor

Ci-VSP, *Ciona intestinalis* voltage-sensing phosphatase

IBMX, 3-Isobutyl-1-methylxanthine

ISO, isoproterenol

mAChR, muscarinic acetylcholine receptor

PMA, phorbol-12-myristate-13-acetate

PIP_2, phosphatidylinositol 4,5-bisphosphate

PKA, protein kinase A

PKC, protein kinase C

Molecular Pharmacology Fast Forward. Published on December 23, 2019 as DOI: 10.1124/mol.119.117192
This article has not been copyedited and formatted. The final version may differ from this version.

Abstract

Smooth muscle cells express Kv7.4 and Kv7.5 voltage-dependent potassium channels, which have each been implicated as regulators of smooth muscle contractility, though they display different sensitivities to signaling via cyclic adenosine monophosphate (cAMP)/protein kinase A (PKA) and protein kinase C (PKC). We expressed chimeric channels composed of different components of the Kv7.4 and Kv7.5 α-subunits in vascular smooth muscle cells to determine which components are essential for enhancement or inhibition of channel activity. Forskolin, an activator of the cAMP/PKA pathway, increased wild-type Kv7.5, but not wild-type Kv7.4 current amplitude. Replacing the amino-terminus of Kv7.4 with the amino-terminus of Kv7.5 conferred partial responsiveness to forskolin. In contrast, swapping carboxy-terminal phosphatidylinositol 4,5-bisphosphate (PIP_2) binding domains, or the entire C-terminus, was without effect on the forskolin response, but the latter conferred responsiveness to arginine-vasopressin (an inhibitory PKC-dependent response). Serine-to-alanine mutation at position 53 of the Kv7.5 amino-terminus abrogated its ability to confer forskolin sensitivity to Kv7.4. Forskolin treatment reduced the sensitivity of Kv7.5 channels to Ci-VSP-induced PIP_2 depletion, whereas activation of PKC with phorbol-12-myristate-13-acetate potentiated the Ci-VSP-induced decline in Kv7.5 current amplitude. Our findings suggest that PKA-dependent phosphorylation of serine 53 on the amino-terminus of Kv7.5 increases its affinity for PIP_2, while PKC-dependent phosphorylation of the Kv7.5 carboxy-terminus is associated with a reduction in PIP_2 affinity; these changes in PIP_2 affinity have corresponding effects on channel activity. Resting affinities for PIP_2 differ for Kv7.4 and Kv7.5, based on differential responsiveness to Ci-VSP activation and different rates of current rundown in ruptured patch recordings.

Significance Statement

Kv7.4 and Kv7.5 channels are known signal transduction intermediates and drug targets for regulation of smooth muscle tone. The present studies identify distinct functional domains that confer differential sensitivities of Kv7.4 and Kv7.5 to stimulatory and inhibitory signaling, and reveal structural features of the channel subunits that determine their biophysical properties. These findings may improve our understanding of the roles of these channels in smooth muscle physiology and disease, particularly in conditions where Kv7.4 and Kv7.5 are differentially expressed.

Introduction

Kv7 family channels mediate a voltage-dependent outward flux of potassium ions, which contributes to the establishment of negative membrane potentials in many cell types. They have well established roles in the regulation of excitability of neurons, cardiac myocytes and smooth muscle cells (Brown and Passmore, 2009; Jespersen et al., 2005; Mackie and Byron, 2008). Kv7 channels are encoded by *KCNQ* genes (1 through 5). The gene products (Kv7.1 – Kv7.5) are the pore-forming α subunits, each of which has 6 membrane-spanning domains (S1-S6) and cytosolic N- and C-termini; functional channels form as homo- or hetero-tetramers of α-subunits (Delmas and Brown, 2005). The prominence of Kv7 channels as regulators of electrical excitability may be ascribed to their unique properties, such as a very negative threshold of activation (negative to -50 mV), absence of time-dependent inactivation, and high sensitivity to signal transduction pathways that influence their probability of opening, either positively or negatively (Delmas and Brown, 2005).

Smooth muscle cells commonly express two functional Kv7 α-subunits, Kv7.4 and Kv7.5, which have different sensitivities to inhibitory and stimulatory signaling (Byron and Brueggemann, 2018). We

Molecular Pharmacology Fast Forward. Published on December 23, 2019 as DOI: 10.1124/mol.119.117192
This article has not been copyedited and formatted. The final version may differ from this version.

recently found that the activity of homomeric Kv7.5, but not homomeric Kv7.4 channels, was strongly enhanced via the activation of the β-adrenergic receptor (β-AR)/Gs/cAMP/PKA pathway and was associated with PKA-dependent phosphorylation of the α subunits (Brueggemann et al., 2018; Mani et al., 2016). A putative PKA phosphorylation site, S53 on amino-terminus of Kv7.5 channel α subunits (but absent from Kv7.4), was implicated in the β-AR-mediated stimulation of channel activity (Brueggemann et al., 2018). How PKA-dependent phosphorylation results in an increase in the open probability of Kv7.5 channels is unknown, nor is it clear whether the lack of an equivalent phosphorylation site on Kv7.4 accounts for its insensitivity to this mode of regulation.

A proposed mechanism by which Kv7 channel activity may be stimulated involves increased binding of phosphatidylinositol 4,5-bisphosphate (PIP_2) to the α-subunits. PIP_2 is a minor membrane phospholipid that associates with Kv7 channels and stabilizes their open state (Gamper and Shapiro, 2007; Suh and Hille, 2008; Zhang et al., 2003). Proposed PIP_2 binding sites include basic residues in S2-S3 linkers, S4-S5 linkers, proximal carboxy-terminus and a more distal carboxy-terminal region located between helices A and B (Choveau et al., 2018; Salzer et al., 2017). All PIP_2 binding sites except this more distal carboxy-terminal region are highly conserved among Kv7 isoforms. Although the amino-termini have not been specifically implicated as PIP_2 binding regions, a proposed mechanism for PKA-dependent enhancement of Kv7.1 channel activity is via phosphorylation of two amino-terminal sites of Kv7.1 α-subunits (Lopes et al., 2007; Marx et al., 2002). PKA-dependent phosphorylation of S27 and S92 was suggested to increase the apparent affinity of the Kv7.1 channel for PIP_2 (Lopes et al., 2007). It has yet to be determined whether equivalent mechanisms underlie the effects of PKA activation on Kv7.5 channels in smooth muscle, or whether a difference in PIP_2 binding affinity renders Kv7.4 less sensitive to PKA-activating stimuli. It is also unknown whether PKC-mediated suppression of Kv7.5 channel activity involves PIP_2 binding, whether it occurs independently of the PKA actions, or if it involves different elements of the channel structure.

In the present study we expressed chimeric channels composed of different components of the Kv7.4 and Kv7.5 α-subunits in vascular smooth muscle cells to determine which structural elements are essential for positive modulation of channel activity by the cAMP/PKA pathway or inhibitory responses to protein kinase C (PKC)-activating stimuli, and to clarify the role of PIP_2 in these processes.

Methods

Constructs. The adenoviral vectors to express human Kv7.4 (Adv-hKv7.4) and Kv7.5 (Adv-hKCNQ5-FLAG) were created previously using the AdEasy Adenoviral Vector System (Stratagene, La Jolla, CA)(Brueggemann et al., 2011). The Ciona intestinalis voltage sensor-containing phosphatase (Ci-VSP) construct was a generous gift of Prof. Yasushi Okamura (Osaka University, Japan). The Ci-VSP cDNA was excised from its original pSD64 vector and was sub-cloned into pICherryNeo vector, a gift from Dario Vignali (Addgene plasmid # 52119). To create chimeric NKv7.5-Kv7.4 channel, the nucleotide sequence of the human KCNQ5 cDNA encoding amino acids 1-53 of Kv7.5 was synthesized by PCR, and used to replace the KCNQ4 sequence encoding the Kv7.4 amino terminus (amino acids 1-55), using restriction sites NheI and BssHII. To create double chimeric channels, NKv7.5-Kv7.4-ΔCKv7.5, the sequence for the PIP_2 binding domain of human KCNQ5 (amino acids 384 to 473) was synthesized by PCR, and cloned into human KCNQ4, to replace amino acids 434 to 521, between restriction sites BsaBI and SacI. To create chimeric channels Kv7.4-CKv7.5 and NKv7.5-Kv7.4-CKv7.5, the carboxy terminal sequence of human KCNQ5 (encoding amino acids Q340 to the end K897) was cloned into human KCNQ4 or into the expression vector

Molecular Pharmacology Fast Forward. Published on December 23, 2019 as DOI: 10.1124/mol.119.117192
This article has not been copyedited and formatted. The final version may differ from this version.

for chimeric NKv7.5-Kv7.4 channels, respectively, to replace the sequence encoding amino acids from Q347 to D695, using restriction site EcoN1. To construct the chimeric channel NKv7.4-Kv7.5, the N-terminal sequence of KCNQ4 (cloned into the pIRES2-EGFP vector) was amplified by PCR to create a BsrG1 restriction site on the 3' end, using primers 5'-GACTTTCCTACTTGGCAGTACATCTAC-3' and 5'-CGTTGTACACCCAGTTCTGCAGG-3'. The 553-base pair PCR product was cloned into TA cloning vector pCR®II according to the manufacturer's protocol (Invitrogen). Subsequently, the KCNQ4- KCNQ5 junction was created by cloning a segment of KCNQ5 (BsrGI-BamHI) into the BsrGI-BamHI restriction sites and DNA sequencing confirmed the in-frame junction. Finally, the full-length sequence for the NKv7.4-Kv7.5 chimera was constructed in pIRES2-EGFP by replacing the Kv7.5 wild type SnaBI-SpeI fragment with the chimeric assembly. Thus, amino acids 1 to 80 of Kv7.5 were replaced by residues 1 to 87 of Kv7.4. All chimeras were confirmed with DNA sequencing. Mutagenesis of the chimeric NKv7.5-Kv7.4 channel was performed using QuikChange Site-Directed Mutagenesis Kit (Agilent). The mutation (serine to alanine) of NKv7.5S53A-Kv7.4 was confirmed by DNA sequencing.

Cell culture. A7r5 cells, an embryonic rat aortic smooth muscle cell line (Kimes and Brandt, 1976), were originally obtained from the ATCC (Byron and Taylor, 1993). A7r5 cells were cultured as described previously (Byron and Taylor, 1993). For overexpression studies, subcultured A7r5 cells at 70% confluence were infected with Adv-hKCNQ5 or Adv-hKCNQ4 at a multiplicity of infection of 100 and used for electrophysiological experiments 7-14 days after infection. Chimeric Kv7 constructs and Ci-VSP were introduced into subcultured A7r5 cells by transient transfection with Lipofectamine 3000® transfection reagent according to the manufacturer's protocol. A7r5 cells expressing chimeric Kv7 channels were used for electrophysiological studies 7-14 days after transfection. For Ci-VSP experiments, A7r5 cells expressing both Kv7.5 channels and Ci-VSP were selected based on the presence of both GFP and mCherry fluorescence, and only those cells which exhibited a detectable Ci-VSP-induced decline in current amplitude in response to applied voltage steps in the range of 0 to +40 mV were used. For Ci-VSP experiments with Kv7.4 channels, detectible Ci-VSP activity at any positive voltages was the criterion for cell selection.

Electrophysiology. Whole cell membrane currents were measured using either a perforated or ruptured patch configuration under voltage-clamp conditions. Note that currents through exogenously expressed Kv7 channels are approximately 100-fold greater in amplitude than native Kv7.5 currents in A7r5 cells (Brueggemann et al., 2009; Brueggemann et al., 2011); the contributions of native Kv7.5 currents to the recordings were therefore deemed negligible. All experiments were performed at room temperature with continuous perfusion of bath solution as described previously (Brueggemann et al., 2007). The standard bath solution for A7r5 cells contained (in mM): 5 KCl, 130 NaCl, 10 HEPES, 2 $CaCl_2$, 1.2 $MgCl_2$, 5 glucose, pH 7.3. Standard internal (pipette) solution for perforated patch experiments contained (in mM): 110 K gluconate, 30 KCl, 5 HEPES, 1 K_2EGTA, pH 7.2. Osmolality was adjusted to 270 mOsm/l with D-glucose. 120 μg/ml Amphotericin B in the internal solution was used for membrane patch perforation. Standard internal (pipette) solution for ruptured patch experiments contained (in mM): 110 K gluconate, 30 KCl, 10 HEPES, 1 K_2EGTA, 1 $MgCl_2$, 0.1 $CaCl_2$, pH 7.2. Osmolality was adjusted to 270 mOsm/l with D-glucose. Voltage-clamp command voltages were generated using an Axopatch 200B amplifier under control of PCLAMP10 software. Series resistances after amphotericin perforation were 8-15 MΩ and were compensated by 60%. Whole-cell currents were digitized at 2 kHz and filtered at 1 kHz respectively. Stable currents were recorded for at least 15 min prior to drug application. Kv7 currents were recorded using a 5 s voltage step protocol from a -74 mV holding potential to test potentials ranging from -124 mV to -4mV

Molecular Pharmacology Fast Forward. Published on December 23, 2019 as DOI: 10.1124/mol.119.117192
This article has not been copyedited and formatted. The final version may differ from this version.

followed by a 1 s step to -120mV. To analyze the voltage-dependence of channel activation the instantaneous tail current amplitude (estimated from exponential fit of current deactivation measured at -120 mV) was converted to conductance according to the equation: $G=I_{tail}/(-120-E_K)$, where I_{tail} is the instantaneous tail current amplitude, -120mV is the tail current step potential and E_K is the reversal potential for potassium (-86mV). Conductance plots recorded in the absence (control) and in the presence of forskolin (1 μM) were fitted to a Boltzmann distribution: $G(V)=G_{max}/[1+exp(V_{0.5}-V)/k]$, where G is conductance, G_{max} is a maximal conductance, $V_{0.5}$ is the voltage of half-maximal activation and k is the slope factor.

For the Ci-VSP experiments, currents through exogenous Kv7.5 channels were measured using a 5-s voltage step protocol from a -74 mV holding potential to test potentials ranging from -120 mV to +120 mV, followed by a 1-s step to -120 mV. Voltage was stepped back to -74 mV for 15 s between test potentials from -120 mV to -20 mV and for 1min between test potentials from 0 mV to +80 mV to allow sufficient time for PIP_2 replenishment. The time course of simultaneous recording of Kv7.5 current modulation and rate of Kv7.5 current decline due to Ci-VSP activation was recorded with a double voltage step protocol: initially voltage was stepped to -20 mV (2.5 s, to test current amplitude at a voltage with no detectible Ci-VSP activity) followed by a 10 s step to +20 mV (for forskolin-treated cells) or to 0 mV (for PMA-treated cells) to measure the rate of current decline due to Ci-VSP activity. Leak was calculated using 200 ms steps to -80 mV and -90 mV in the beginning of each protocol and subtracted off line. This double voltage step protocol was repeated every 1 min to allow sufficient time for PIP_2 replenishment. Currents were recorded for 5 min prior drug application to ensure recording stability. Rates of the current decline due to Ci-VSP activity were calculated based on linear regression of the time courses of current recordings in response to +20 mV or 0 mV steps, and are presented as % of current decline per second.

Time courses of Kv7.5 and Kv7.4 current rundown were recorded in the whole-cell ruptured patch configuration by applying 5 s voltage steps to -20 mV every 15 s; the voltage protocol was started 1 min after establishing the whole-cell configuration. To measure the rate of wortmannin-induced decline of endogenous Kv7.5 current amplitude, current was recorded at -20 mV holding voltages for 15 min before wortmannin application, and for an additional 15 min in the presence of 10 μM wortmannin in the bath solution, with or without forskolin (1 μM) and 3-Isobutyl-1-methylxanthine (IBMX, 500 μM). Current traces were normalized by the average current value at -20 mV measured during the last 5 min before wortmannin application; rate of current decline was estimated based on linear regression of the current measured during last 5 min of wortmannin application, and presented as % decline per min.

Membrane [PIP_2] assay. The effects of various treatments on membrane PIP_2 abundance was measured using a Green Down PIP_2 sensor (Green Fluorescent Live Cell PIP_2 Assay Kit; Montana Molecular, Cat# D0400G). Briefly, A7r5 cells were infected with BacMam viruses encoding the Green Down PIP_2 sensor along or with HM1 Muscarinic Receptor BacMam (for positive control) and plated on 8 chamber borosilicate coverglass slides (Lab-Tek, Rochester, NY). Expression of PIP_2 sensor was confirmed based on presence of green fluorescence (GFP excitation wavelengths), expression of HM1 receptors was confirmed based on presence of red nuclear label. A7r5 cells were used for experiments 72 hr after infection. A7r5 cells expressing PIP_2 sensor with or without HM1 receptors were imaged as described previously with an inverted microscope (Nikon Eclipse TE2000-U) equipped with a metal halide lamp and a back-thinned CCD camera (iXon 887: Andor Technology, Belfast, Northern Ireland) (Raguimova et al., 2018). For each field containing 1- 6 fluorescent cells, images were acquired every 5 s using 40x objective at 488/25 nm excitation, 510/30 nm emission wavelengths using MetaMorph software

Molecular Pharmacology Fast Forward. Published on December 23, 2019 as DOI: 10.1124/mol.119.117192
This article has not been copyedited and formatted. The final version may differ from this version.

(Molecular Devices, Sunnyvale, CA) for 2 min before addition of the treatment and for additional 8 min after treatment. Stacks of images were analyzed with ImageJ software. Average background fluorescence measured in a region of the image that contained no cells was subtracted frame by frame from the measurements of the mean pixel values of the fluorescent cells. Fluorescence intensity of each frame was normalized by average fluorescence intensity measured within 2 min period before treatment for every cell. Each n represents an individual cell; for each treatment condition 4-6 fields were analyzed from 2-3 independent experiments.

Statistics. Data were analyzed using SigmaPlot (Systat Software, Inc., San Jose, CA USA). Data are expressed as mean ± standard deviation (S.D.) to provide an indication of variability in the original sampled population. Sample size for each group was not pre-determined, but instead was based on effect size and intrinsic variability within each group under the recording and treatment conditions that were applied. Two-tailed paired Student's *t*-test was used to compare parameters measured before and after treatments. For comparisons between two independent groups, two-tailed *t*-test was used. Differences among multiple treatment groups were assessed by analysis of variance (ANOVA) followed by a Holm-Sidak post hoc test. Differences were considered statistically significant with p values ≤ 0.05. All groups were included in multiple groups ANOVA testing with no exceptions and results from all performed inter-group comparisons are reported irrespective of outcome.

Materials. Cell culture media were from MediaTech (Herndon, VA, USA). Fetal bovine serum was from Atlanta Biologicals. Amphotericin B, 3-Isobutyl-1-methylxanthine (IBMX), phorbol-12-myristate-13-acetate (PMA), 4α-phorbol-12-myristate-13-acetate (4αPMA), isoproterenol (ISO), arginine- vasopressin (AVP) were from Sigma-Aldrich (St. Louis, MO, USA). Forskolin was from Tocris Bioscience (Minneapolis, MN, USA). Wortmannin was from Selleck Chemicals (Houston, TX, USA). The AdEasy Adenoviral Vector System was from Stratagene. The QuikChange Site-Directed Mutagenesis Kit was from Agilent Technologies (Santa Clara, CA, USA). The human *KCNQ5* cDNA (accession number: AF202977, originally in the insect cell expression vector pMT) was a generous gift from Dr. T. Jentsch at the Max-Delbrück-Centrum for Molecular Medicine (Berlin, Germany). The human KCNQ4 cDNA (accession number: AF105202, originally in the mammalian expression vector pMT) was a generous gift from Dr. Ian Wood at the University of Leeds, Leeds, UK. Green Down PIP_2 sensor BacMam was from Montana Molecular (Bozeman MT, USA).

Results

Previously we provided evidence that activation of the βAR/cAMP/PKA pathway leads to enhancement of Kv7.5 activity and that serine 53 located on the amino terminus of Kv7.5 channels is an essential PKA phosphorylation site (Brueggemann et al., 2018). In agreement with the previous findings, current through exogenous human Kv7.5 channels expressed in A7r5 vascular smooth muscle cells was significantly enhanced by forskolin (1 μM), a direct activator of the cAMP/PKA pathway (Fig. 1Aii). The increase in amplitude of Kv7.5 current was not associated with a significant shift of the activation curve ($V_{0.5}$=-45.2 ± 3.8 mV in control and $V_{0.5}$=-51.3 ± 9.1 mV in the presence of forskolin, n=4, p = 0.17, Student's *t*-test, Fig. 1 Aiii).

In contrast to Kv7.5, exogenously expressed human Kv7.4 channels were insensitive to forskolin (Fig. 1Bii, Biii). We tested whether we could confer sensitivity of Kv7.4 channels to activation of the

Molecular Pharmacology Fast Forward. Published on December 23, 2019 as DOI: 10.1124/mol.119.117192
This article has not been copyedited and formatted. The final version may differ from this version.

cAMP/PKA pathway by replacing its amino-terminus with the amino-terminus of the Kv7.5 channel. The NKv7.5-Kv7.4 chimeric construct (Fig. 1Ci) formed functional channels with voltage-dependence of activation similar to wild-type Kv7.4 channels ($V_{0.5}$=-33.9 ± 3.4 mV, n=5, for Kv7.4 and $V_{0.5}$=-31.5 ± 4.1 mV, n=10, for NKv7.5-Kv7.4, Fig. 1B, C, Fig. 2B), but like Kv7.5, the current was significantly enhanced by forskolin (1 μM, Fig. 1C, Fig. 2A). Notably, the forskolin-induced enhancement of current through chimeric NKv7.5-Kv7.4 channels (28.6± 9.9% increase in current amplitude at -20 mV, n=5) was significantly less than that observed for wild-type Kv7.5 channels (61.3± 13.4% increase in current amplitude at -20 mV, n=4; Fig. 2A). The response to forskolin treatment was critically dependent on the presence of serine 53 on the amino terminus: mutation of serine 53 to alanine abolished forskolin-induced enhancement of current through chimeric NKv7.5**S53A**-Kv7.4 channels (3.5± 12.3% increase in current amplitude at -20 mV, n=4; Fig. 2).

We hypothesized that the result of cAMP/PKA activation is increased binding of PIP_2 to Kv7.5 channels, which in turn increases the open probability of the channels. Given that the PIP_2 binding region located between helices A and B on the carboxy-terminal is the least conserved PIP_2 binding region between Kv7.4 and Kv7.5 (Zaydman and Cui, 2014), this region might contribute to the apparent differences in their sensitivities to forskolin. To test this hypothesis, we further modified the NKv7.5-Kv7.4 chimeric channel by replacing the carboxy-terminal PIP_2 binding region located between helices A and B of Kv7.4 with the corresponding region of Kv7.5, creating a new double chimeric channel (see schematic in Fig. 1Di). The resulting NKv7.5-Kv7.4-ΔCKv7.5 chimeric construct formed functional channels with voltage-dependence of activation similar to wild-type Kv7.4 channels, but with a slight positive shift of the activation curve ($V_{0.5}$=-33.9 ± 3.4 mV, n=5 for Kv7.4 and $V_{0.5}$=-27.8 ± 1.9 mV, n=4 for NKv7.5-Kv7.4-ΔCKv7, n=4, P=0.015, Student's *t*-test, Fig. 1B, D, Fig.2B). Its current was significantly enhanced by forskolin (1 μM; 32.2 ± 7.8% increase in current amplitude at -20 mV, n=4) to approximately the same extent as NKv7.5-Kv7.4 chimeric channel, and less than wild-type Kv7.5 channels.

To test whether the more robust PKA-dependent potentiation of Kv7.5 channels requires interaction of the amino terminus with the intact Kv7.5 carboxy terminus, we created new double chimeric channels containing both amino and carboxy termini of Kv7.5, but with membrane spanning domains of the Kv7.4 channel (see schematic in Fig. 1Ei). The resulting NKv7.5-Kv7.4-CKv7.5 chimeric construct formed functional channels. Surprisingly, the voltage-dependence of activation of NKv7.5-Kv7.4-CKv7.5 channels was similar to wild-type Kv7.5 channels rather than Kv7.4 channels ($V_{0.5}$=-48.4 ± 7.7 mV, n=6 for NKv7.5-Kv7.4-CKv7.5 and $V_{0.5}$=-45.2 ± 3.8 mV, n=4 for Kv7.5, n=4, Fig. 1A, E, Fig.2B). Current through NKv7.5-Kv7.4-CKv7.5 channels was enhanced by forskolin (1 μM) to approximately the same extent as through NKv7.5-Kv7.4 chimeric channel, but less than wild-type Kv7.5 current (25.8± 7.3% increase in current amplitude at -20 mV, n=4, Fig. 1Eii, 2A).

To test whether the full carboxy terminus of Kv7.5 alone would be sufficient to shift voltage-dependence of activation of Kv7.4 channels to a more negative range, we created yet another chimeric construct, replacing just the carboxy terminus of Kv7.4 with the carboxy terminus of Kv7.5 (see schematic on Fig. 1Fi). The resulting Kv7.4-CKv7.5 chimeric construct formed functional channels with voltage-dependence of activation similar to wild-type Kv7.5 channels ($V_{0.5}$=-41.6 ± 3.7 mV, n=9 Fig. 1F, Fig.2B), but which were insensitive to forskolin (1 μM) (Fig. 1Fii, 2A).

We further explored the structural determinants of forskolin-stimulated current potentiation and voltage-dependence of activation by creating a reverse chimera, replacing the amino terminus of Kv7.5

Molecular Pharmacology Fast Forward. Published on December 23, 2019 as DOI: 10.1124/mol.119.117192
This article has not been copyedited and formatted. The final version may differ from this version.

with the amino terminus of Kv7.4. (see schematic in Fig. 1Gi). The resulting NKv7.4-Kv7.5 chimeric construct formed functional channels with voltage-dependence of activation similar to wild-type Kv7.5 channels ($V_{0.5}$=-41.5 ± 2.9 mV, n=9 Fig. 1G, Fig.2B), but which were completely insensitive to forskolin (1 μM) (Fig. 1Gii, 2A).

Our previous findings, also using A7r5 cells as an expression system, revealed that wild-type human Kv7.5 currents are enhanced by activation of G_s-coupled receptors and suppressed in response to activation of $G_{q/11}$-coupled receptors; in contrast, wild-type human Kv7.4 currents are insensitive to either of these stimuli (Brueggemann et al., 2014; Mani et al., 2016). To explore the structural determinants of these differential regulatory sensitivities, we tested the effects of activation of each of these signaling pathways on chimeric Kv7.4-Kv7.5 channel constructs with amino or carboxy termini switched. Currents through NKv7.5-Kv7.4 chimeric channels were slightly enhanced (24.1 ± 15.2%, n=7) in response to application of G_s-coupled βAR agonist isoproterenol (1 μM), though this effect was significantly less than enhancement of wild-type Kv7.5 currents (168.1 ± 44.2%, n=5) and not different from enhancement of wild-type Kv7.4 current (22.4 ± 15.4%, n=6) or current through Kv7.4-CKv7.5 chimeric channels (12.9 ± 7.5%, n=5; Fig. 3 A, B, D). In contrast, currents through Kv7.4-CKv7.5 chimeric channels were significantly suppressed by $G_{q/11}$-coupled V_{1a} receptor agonist arginine vasopressin (AVP, 100 pM; 35.6 ± 23.1% reduction in current amplitude, n=7, Fig 3. A, B, E), though to a lesser extent then wild-type Kv7.5 channels (66.2 ± 21.4% reduction in current amplitude, n=9, Fig. 3E); NKv7.5-Kv7.4 chimeric channels were insensitive to AVP. Chimeric construct NKv7.4-Kv7.5 was insensitive to isoproterenol (1 μM) and was regulated to the same extent as wild-type Kv7.5 channels by AVP (application of 100 pM AVP reduced current amplitude by 61.5 ± 25.8%, n=7; Fig. 3 C, E).

Considering that our findings indicate that G_s/cAMP/PKA signaling to Kv7.5 depends to some extent on the amino terminus of the channel, whereas sensitivity to the $G_{q/11}$/PKC pathway depends on the carboxy terminus, we examined the effects of these pathways on the affinity of Kv7.5 for PIP_2. We expressed Ci-VSP, a voltage-sensing phosphatase (Iwasaki et al., 2008), in A7r5 cells as a tool for manipulating the membrane level of PIP_2. Activation of Ci-VSP causes de-phosphorylation and thus voltage-dependent reduction of membrane [PIP_2] (Iwasaki et al., 2008). We found that activation of Ci-VSP at voltages positive to 0 mV induced a time- and voltage-dependent decline in Kv7.5 current amplitude (Fig. 4; this only occurred in cells co-expressing Ci-VSP—current amplitude was stable when the same voltage steps were applied in cells expressing Kv7.5 alone (Supplemental Fig. 1)). In the presence of forskolin (1 μM), the rate of the Ci-VSP-induced current decline was significantly decreased (from 8.8 ± 3.7 min to 6.0 ± 4.3 min, n=3, P=0.024, paired Student's *t*-test, Fig. 4 A-C), suggesting an increase in the affinity of the channel for PIP_2. The decrease of the current decline rate measured at +20 mV and the increase in the current amplitude measured at -20 mV (voltage without detectable Ci-VSP activity) occurred with similar time courses ($t_{0.5}$= 3.5 ± 1.3 min for the decrease in Ci-VSP-induced rate of current decline, and 3.8 ± 1.5 min for the increase in current amplitude after forskolin application, n=3, P=0.353, paired Student's *t*-test, Fig. 4B). Application of forskolin (1 μM) did not induce a positive shift of the voltage at which a Ci-VSP induced Kv7.5 current decline was observed (Fig. 4D), nor did it affect the rate of decline in currents recorded from cells expressing NKv7.4-Kv7.5 chimeric channels (Fig. 4E-F), supporting the interpretation that the effects on wild-type Kv7.5 currents are due to altered PIP_2 binding rather than an effect of forskolin on Ci-VSP activity.

To achieve maximal activation of the cAMP-PKA pathway we used a combination of 10 μM forskolin and phosphodiesterase inhibitor 3-Isobutyl-1-methylxanthine (IBMX, 500 μM). In the presence

Molecular Pharmacology Fast Forward. Published on December 23, 2019 as DOI: 10.1124/mol.119.117192
This article has not been copyedited and formatted. The final version may differ from this version.

of forskolin/IBMX, a 2.5-fold increase of the Kv7.5 current amplitude was measured at -20 mV; this was associated with a robust positive shift of the threshold voltage at which Ci-VSP induced a decline in Kv7.5 current amplitude (from 13 ± 15 mV to 62 ± 33 mV, P= 0.03, n=5, paired Student t-test; Fig. 5 A, B). The Ci-VSP-induced decline in current amplitude measured at +20 mV was completely abolished after application of forskolin/IBMX for 5 min, (from 12.5 ± 7.0%/s before to 0.5 ± 2.1%/s following treatment; P=0.007, n=6, paired Student's t-test). We also tested forskolin/IBMX treatment on native Kv7.5 currents in A7r5 cells (Kv7.5 is the only Kv7 channel subtype natively expressed in A7r5 cells (Brueggemann et al., 2011; Brueggemann et al., 2007)) using an alternative strategy to monitor PIP_2 affinity. In this case, wortmannin treatment was applied to decrease PIP_2 levels. Wortmannin, at micromolar concentrations, is known to inhibit the activity of phosphatidylinositol-4 kinase, which is necessary for replenishment of membrane [PIP_2], thus eventually causing membrane PIP_2 depletion (Suh and Hille, 2002; Zhang et al., 2013). Wortmannin (10 μM) reduced endogenous Kv7.5 current recorded at -20 mV holding voltage (current amplitude was stable in the absence of wortmannin, but declined at a rate of 3.5 ± 0.7 %/min during wortmannin treatment; Fig. 5C). Application of forskolin (1 μM) with IBMX (500 μM) enhanced the endogenous Kv7.5 current amplitude by 5 -fold and significantly reduced the rate at which Kv7.5 current declined in response to wortmannin treatment (to 1.7 ± 1.1 %/min, P= 0.03, n=4, Student's t-test), supporting an increased affinity of the native Kv7.5 channels for PIP_2 following treatment with forskolin/IBMX.

To test whether the inhibitory G_q-coupled receptor-mediated effects are the result of a PKC-dependent *decrease* in the apparent PIP_2 affinity of the Kv7.5 channels, we measured the rate of the Ci-VSP- induced Kv7.5 current decline using 10 s steps to 0 mV before and during treatment with PMA (1 nM), a direct activator of PKC. PMA induced a gradual reduction of the Kv7.5 current amplitude (measured as relative current amplitude at -20 mV) and an increase in the rate of the Ci-VSP-induced Kv7.5 current decline (from 2.2 ± 2.7 %/s to 4.5 ± 3.8 %/s, n=7, P= 0.015, paired Student's t-test); these effects occurred with similar time courses ($t_{0.5}$= 8.6 ± 2.6 min for the decrease in current amplitude and $t_{0.5}$= 7.2 ± 2.0 min for the increased rate of the Ci-VSP-induced Kv7.5 current decline after PMA application, n=7, P=0.228, paired Student's t-test, Fig. 6 A-C). Activation of PKC with PMA (1 nM) did not result in a significant negative shift of Ci-VSP induced Kv7.5 current decline (Fig. 6 D). An inactive analog of PMA, 4αPMA (1 nM) did not suppress Kv7.5 current measured at -20 mV and did not significantly affect Ci-VSP-induced Kv7.5 current decline (rate of current decline was 1.2 ± 1.6%/s before and 1.9 ± 1.7%/s after 4αPMA application for 15 min, n=5, P=0.335, paired Student's t-test, data not shown).

Treatments that target physiological signaling pathways might affect PIP_2 abundance as well as PIP_2 affinity for Kv7 α-subunits. To determine whether membrane [PIP_2] was altered under our treatment conditions, we used a green fluorescent membrane PIP_2 sensor (see *Methods*) to monitor changes in membrane [PIP_2] over time under similar treatment conditions (Fig. 7). As shown in Fig. 7A, treatments with 10 μM forskolin/500 nM IBMX or with 1 nM PMA had no more effect than a vehicle control, whereas a muscarinic acetylcholine receptor agonist, carbachol, revealed a robust loss of PIP_2 from the membrane in A7r5 cells overexpressing M1 muscarinic acetylcholine receptors. AVP, at a physiological concentration that robustly suppresses wild-type Kv7.5 currents (100 pM, Fig. 3E), did not detectably alter membrane [PIP_2], whereas higher concentrations (1 nM, 10 nM) did induce a concentration-dependent decrease in [PIP_2] (Fig. 7B).

Some differences in sensitivities of Kv7 channels to physiological stimuli might arise as a result of differences in *resting* PIP_2 affinities, i.e. the affinity for PIP_2 in the absence of a regulatory stimulus. PIP_2

Molecular Pharmacology Fast Forward. Published on December 23, 2019 as DOI: 10.1124/mol.119.117192
This article has not been copyedited and formatted. The final version may differ from this version.

affinities were previously compared among Kv7.2-Kv7.4 homomeric channels and Kv7.2/7.3 heteromeric channels (Li et al., 2005), but Kv7.5 was not included in that study. To compare relative PIP_2 affinities of Kv7.4 and Kv7.5 channels in vascular smooth muscle cells, we measured voltage-dependent suppression of Kv7.4 or Kv7.5 current amplitude in cells expressing Ci-VSP. The effects of Ci-VSP activation on current amplitude were strikingly different for Kv7.4 and Kv7.5, with a clear voltage-dependent suppression of Kv7.5 starting at voltages positive to 0 mV, but little or no suppression of Kv7.4 currents at voltages up to +80 mV (Fig. 8A). We also examined time courses and extent of current rundown using a ruptured patch configuration. Kv7.5 current tended to run down faster than Kv7.4 current (τ= 4.6 ± 2.5 min, n=13 for Kv7.5 current, τ= 9.1 ± 9.3 min, n=15 for Kv7.4 current, P=0.182 Mann-Whitney Rank Sum test). The extent of Kv7.5 current rundown was greater than Kv7.4 current rundown (76.7 ± 14.6% reduction in Kv7.5 current amplitude in 10 min, n=13, 55.2 ± 18.9% reduction in Kv7.4 current amplitude in 10 min, n=15, P=0.003, Student's t-test, Fig. 8B,C). Forskolin (10 µM) in combination with IBMX (500 µM) significantly reduced the extent of Kv7.5 current rundown in ruptured patch recordings (from 76.7 ± 4%, n=13, to 38.7 ± 4%, n= 8, reduction in current amplitude in 10 min, P< 0.001, Student's t-test, Fig. 7B). There was no effect of this same treatment on Kv7.4 current rundown in ruptured patch recordings (50.5 ± 8% reduction in current amplitude in 10 min, n=7, P=0.615, Student's t-test, Fig. 8C).

Discussion

Our previous studies suggested that increased phosphorylation of Kv7.5 α-subunits in vascular or airway smooth muscle cells can result in either an increase in channel activity (PKA-dependent) or a decrease in channel activity (PKC-dependent); Kv7.4 α-subunits were insensitive to either mode of regulation (Brueggemann et al., 2018; Brueggemann et al., 2014; Haick et al., 2017; Mani et al., 2016). The mechanism by which PKC- or PKA-dependent phosphorylation modulates Kv7.5 channel activity, and the basis for the difference between Kv7.4 and Kv7.5, remained unknown. Our present findings suggest that changes in PIP_2 affinity, as a result of G_s- or $G_{q/11}$-coupled receptor activation, may be responsible for the resulting increase or decrease in Kv7.5 channel activity following agonist treatments. Furthermore, the results suggest that structural elements responsible for altering PIP_2 affinity are not within previously identified conserved PIP_2 binding domains, but instead involve phosphorylation sites on the cytosolic N- and C-termini of Kv7.5 that are targeted specifically by PKA and PKC, respectively, with opposite consequences in terms of PIP_2 affinity and channel activity. Kv7.4 α-subunits lack the crucial PKA and PKC phosphorylation sites, and homomeric Kv7.4 channels have a higher resting affinity for PIP_2, which may account for their relative insensitivity to G_s- or $G_{q/11}$-coupled receptor signaling via PKA and PKC, respectively.

Previous evidence that activation of the βAR/cAMP/PKA pathway leads to enhancement of Kv7.5 activity and that serine 53 located on the amino terminus of Kv7.5 channels is an essential PKA phosphorylation site includes: 1) the increased amplitude of natively expressed smooth muscle Kv7.5 currents or currents via exogenously expressed human Kv7.5 in response to formoterol, a βAR agonist, or rolipram (a cAMP phosphodiesterase inhibitor) was prevented by treatment with a PKA inhibitor; 2) isoproterenol (another βAR agonist) stimulated phosphorylation of human Kv7.5 (but not Kv7.4), as detected by an anti-phosphoserine PKA substrate antibody in proximity ligation assays, and this was prevented by pretreatment with a PKA inhibitor; 3) phosphoproteomic analysis of Kv7.5 amino acid sequence identified S53 as a putative PKA phosphorylation site; 4) mutation of S53 to alanine (S53A) inhibited forskolin-induced enhancement of Kv7.5 current (Brueggemann et al., 2018; Mani et al., 2016). In agreement with the previous findings, we report here that forskolin (1 µM), a direct activator of the cAMP/PKA pathway, significantly enhanced current through exogenous human Kv7.5 channels expressed in A7r5 cells, and the

Molecular Pharmacology Fast Forward. Published on December 23, 2019 as DOI: 10.1124/mol.119.117192
This article has not been copyedited and formatted. The final version may differ from this version.

increase in amplitude of Kv7.5 current was not associated with a significant shift of the activation curve, similar to previously observed effects of isoproterenol on native Kv7.5 currents or currents via exogenously expressed Kv7.5 channels in A7r5 cells (Mani et al., 2016).

Relatively little is known regarding how the N-termini function as regulators of the open probability of Kv7 channels. Though there is considerable heterogeneity in this region among the five Kv7 α-subunit subtypes, there is evidence that some of the N-termini can participate in cAMP/PKA-mediated signal transduction. For example, there is proteomic evidence for PKA-dependent phosphorylation of amino-terminal residue S52 of Kv7.2 (Erdem et al., 2017), and functional evidence that phosphorylation at this site has a potentiating effect on current amplitude (Schroeder et al., 1998), as we have proposed for phosphorylation of S53 of Kv7.5. In the absence of any treatment, the N-terminus of Kv7.2 was proposed to have an inhibitory effect on current amplitude, based on chimeric constructs with interchanged domains of Kv7.2 and Kv7.3 α-subunits (Etxeberria et al., 2004). A PKA phosphorylation site was identified at S27 on the N-terminus of the Kv7.1 α-subunit and proposed to account for observed cAMP/PKA-mediated increases of Kv7.1 current amplitude (Boucherot et al., 2001; Marx et al., 2002). However, though the N-terminal tail was found to be necessary for PKA-dependent regulation of Kv7.1, mutation of S27 to alanine did not prevent the response (Boucherot et al., 2001).

Our findings suggest that differential phosphorylation likely contributes to the different functional responses of Kv7.4 and Kv7.5 to PKA-activating stimuli. In a predominantly Kv7.4 channel, but in which the N-terminal tail of Kv7.4 was replaced with that from Kv7.5, we observed a partial responsiveness to a PKA-activating stimulus, but this responsiveness was lost if the putative PKA phosphorylation site, S53 on the Kv7.5 N-terminus, was mutated to alanine. Thus, part of the response appears to be dependent on phosphorylation of S53, which is normally absent from Kv7.4. Although replacement of the Kv7.4 N-terminus with that from Kv7.5 conferred significant responsiveness to forskolin (Fig. 2), this NKv7.5-Kv7.4 construct displayed a very weak response to isoproterenol (Fig. 3), raising the possibility that βAR activation is a weaker stimulus for PKA-dependent phosphorylation of S53, or that additional receptor-mediated signaling events attenuate the measured response. Previous research has suggested that activation of βARs leads to activation of Kv7.4 via direct interactions of the channel proteins with the βγ-subunits of heterotrimeric G proteins (Stott et al., 2015). It is not clear how this mechanism might affect PKA-dependent stimulation of a chimeric channel with the N-terminus of Kv7.5 and the remainder of the structure derived from Kv7.4.

The effect of PKA-dependent phosphorylation may be attributable to increased PIP_2 affinity for Kv7.5, based on our Ci-VSP results—the higher the apparent affinity of a channel for PIP_2, the less susceptible it is to the rapid removal of PIP_2 from the membrane (Gamper and Shapiro, 2007; Salzer et al., 2017). Our results clearly show that the effect of Ci-VSP-induced PIP_2 hydrolysis is markedly reduced following treatments that activate the cAMP/PKA pathway. Notably, the time course of the apparent change in PIP_2 affinity mirrored the time course for forskolin-induced enhancement of the current. If PKA-dependent phosphorylation of S53 on Kv7.5 enhances the currents by increasing the channel's affinity for PIP_2, why is the forskolin-induced increase in NKv7.5-Kv7.4 less than that observed with wild-type Kv7.5? Perhaps a complete replacement of the N-terminus would have conferred full responsiveness (we only replaced the first 53 amino acids). Another possibility is that, even if NKv7.5-Kv7.4 is phosphorylated on the same residue, the core structure of Kv7.4 already has a relatively high resting affinity for PIP_2—the change in phosphorylation state may have less impact on PIP_2 binding or its ability to regulate Kv7.4 pore opening. The differences in sensitivity to Ci-VSP activation between Kv7.4 and Kv7.5 suggest that, even in the absence of any treatment, WT Kv7.4 and WT Kv7.5 differ substantially in their affinities for PIP_2. This is further supported by the observed differences in time/extent of rundown of currents in ruptured patch recordings; rundown rates likely reflect the rate of dissociation of PIP_2 from the channel as PIP_2 levels

Molecular Pharmacology Fast Forward. Published on December 23, 2019 as DOI: 10.1124/mol.119.117192
This article has not been copyedited and formatted. The final version may differ from this version.

decline (Suh and Hille, 2008). Both sets of results suggest that Kv7.4 has a much higher affinity for PIP_2 compared with Kv7.5.

The reduced sensitivity of Kv7.4 to cAMP/PKA-activating stimuli, even when its N-terminus was replaced with the N-terminus of Kv7.5 (NKv7.5-Kv7.4) cannot be attributed to differences in the least conserved PIP_2 binding domain on the C-terminus, because replacing that domain of Kv7.4 with the corresponding domain from Kv7.5 had no further impact on the response to forskolin. Other PIP_2 binding domains are highly conserved among all of the Kv7 family members. Thus, it may be differences in the remaining core structure of Kv7.5 that confer decreased resting affinity to PIP_2 and that dictate its sensitivity to PKA-dependent signaling. The idea that the core structure is a primary determinant of PIP_2 affinity and sensitivity to signaling events is further supported by the observation that the effect of AVP was reduced in a construct that had only the C-terminus of Kv7.5 (Kv7.4-NKv7.5) compared with its effect on WT Kv7.5 or NKv7.4-Kv7.5 currents (having the core Kv7.5 structure appears to be essential for the full PKC-dependent suppression of Kv7.5 current, which may be attributable to decreased PIP_2 affinity (see below)).

It has not been clearly established how phosphorylation of Kv7 α-subunit N-termini contribute to PIP_2 binding affinities. The transfer of a negatively charged phosphate moiety onto a serine residue would be expected to alter the local electrostatic environment, which might account for its ability to affect binding of PIP_2, which has a negatively charged head group (McLaughlin et al., 2002; Suh and Hille, 2008). This perhaps over-simplified explanation of our experimental results may find some support from an examination of the amino acid sequences upstream and downstream of the Kv7.5 S53 substrate, which includes multiple basic residues (14 arginines, 4 lysines, and 1 histidine within the surrounding cytosolic N-terminal segment). It has been suggested previously that alterations in localized electrostatic interactions within protein structures might lead to lateral reorganization of the multivalent PIP_2 or more directly affect the lipid-protein interactions (McLaughlin et al., 2002). We speculate that, in the context of the 3-dimensional structure of the tetrameric channel, these electrostatic effects on the N-termini might impact the PIP_2 within the membrane surrounding the channel structure or its interaction with regions in the S2-S3 linkers, S4-S5 linkers, and carboxy-terminal regions previously identified as conserved PIP_2-binding domains (Choveau et al., 2018); the ultimate consequence would be an increase in channel activity.

Previous studies of Kv7.2 regulation have focused on phosphorylation sites within the C-terminal PIP_2 binding regions, revealing that phosphorylation in this region can *reduce* PIP_2 binding affinity; additional evidence suggested that phosphorylation at these sites is essential for the suppression of Kv7.2 currents in response to $G_{q/11}$-coupled M1 muscarinic acetylcholine receptor (mAChR) activation (Salzer et al., 2017). We found that replacing the C-terminal Kv7.4 PIP_2 binding regions, or even the entire cytosolic C-terminus, with corresponding Kv7.5 sequences did not confer responsiveness to forskolin/IBMX. Based on these results, we conclude that the differential responsiveness of Kv7.4 and Kv7.5 to PKA-activating stimuli is not attributable to differential phosphorylation of residues on the C-terminus. On the other hand, consistent with the findings of Salzer *et al.* (Salzer et al., 2017), our results suggest that the C-termini of Kv7.4 and Kv7.5 do appear to be the source of differential responsiveness with regard to PKC-dependent suppression of channel activity and its associated reduction in PIP_2 affinity: replacing the C-terminus of Kv7.4 with that from Kv7.5 did confer sensitivity to a PKC-activating stimulus (AVP).

Earlier work by Hoshi and colleagues suggested that suppression of Kv7.2 current in response to activation of M1 muscarinic acetylcholine receptors involves PKC activation and consequent phosphorylation of the C-terminus at position serine 541 (Hoshi et al., 2003). Subsequent research provided evidence that this phosphorylation of S541, which is located on or near a calmodulin-binding domain on the Kv7.2 α-subunit

Molecular Pharmacology Fast Forward. Published on December 23, 2019 as DOI: 10.1124/mol.119.117192
This article has not been copyedited and formatted. The final version may differ from this version.

C-terminus, results in dissociation of calmodulin, which reduces the affinity of Kv7.2 for PIP_2 and thereby suppresses channel activity (Kosenko et al., 2012). Our present findings support a similar effect of PKC phosphorylation of Kv7.5 α-subunits, i.e. a reduction in their affinity for PIP_2 and suppression of channel activity. We observed that the time course for the apparent PKC-mediated decrease in PIP_2 affinity mirrored the time course for suppression of Kv7.5 current. We previously implicated S441 as the PKC phosphorylation site on the Kv7.5 C-terminus that mediates PKC-dependent suppression of channel activity in airway smooth muscle cells (Haick et al., 2017). That site is more membrane proximal than the calmodulin binding domain where S541 resides on Kv7.2. It is therefore unclear whether the mechanisms are the same for PKC-dependent regulation of Kv7.2 and Kv7.5, though in both cases the ultimate effects appear to be decreased PIP_2 binding and reduced channel opening. Our findings further suggest that Kv7.4 α-subunits lack the PKC-sensitive signaling elements, but can respond to PKC activation with a reduction of channel activity if the Kv7.5 C-terminus is inserted in place of its own C-terminus.

The Ci-VSP results provide an indirect measurement of Kv7 channel PIP_2 affinity, and do not rule out effects of treatments on membrane PIP_2 abundance. Our independent assessment of membrane PIP_2 abundance using a fluorescent PIP_2 sensor suggests that, at the concentrations which altered Ci-VSP responses, neither the cAMP/PKA-activating stimuli nor the PKC-activating stimuli appreciably altered membrane PIP_2 levels. Admittedly, we cannot rule out the possibility that changes in PIP_2 abundance occur in micro- or nano-domains that are not detected by the sensor, though it appears there is a vast total reserve of PIP_2 in the membrane that can be cleaved in response to a maximal activation of G_q-coupled receptors. In addition to Ci-VSP, we used two other well-established, but also admittedly indirect, strategies to evaluate PIP_2 affinity: wortmannin, and rundown of whole cell currents in ruptured patch recordings. Both of these approaches yielded results that converge with the Ci-VSP results, supporting the hypothesis that the treatments altered the PIP_2 affinity of the channels. We therefore conclude that the most likely explanation for our findings is that cAMP/PKA-mediated enhancement and PKC-mediated suppression of Kv7.5 currents are associated with an increase or a decrease in PIP_2 affinity, respectively. These signaling events appear to involve different elements of the channel structure and can occur independently of one another.

Another perhaps unexpected finding of our study was that the cytosolic C-terminal domains of Kv7.4 and Kv7.5 appear to dictate the voltage dependence of channel activation. We found that $V_{0.5}$ values of WT Kv7.4 were >10 mV more positive than WT Kv7.5, as reported previously (Brueggemann et al., 2014; Brueggemann et al., 2011; Mani et al., 2016), and chimeric channels generally exhibited $V_{0.5}$ values that corresponded to whichever C-terminus was expressed (constructs with the Kv7.5 C-terminus had $V_{0.5}$ negative to -40 mV, whereas those with the Kv7.4 C-terminus had significantly more positive $V_{0.5}$ values, closer to -30 mV.

In summary, the present research findings reveal that distinct functional domains are responsible for differential sensitivities of Kv7.4 and Kv7.5 channels to stimulatory and inhibitory signaling via PKA and PKC, respectively. The results further suggest that Kv7.4 and Kv7.5 exhibit fundamental differences in their PIP_2 affinities and differences in their C-termini that determine their voltage-dependence of activation, even in the absence of stimuli. We speculate that some vascular and airway diseases may involve altered regulation of Kv7 channel function via changes in expression or stoichiometry of Kv7.4/Kv7.5 α-subunits. For example, hypoxia was reported to result in downregulation of Kv7.4, but not Kv7.5, channels in the pulmonary vasculature (Sedivy et al., 2015). The result, based on our present findings, may be increased abundance of Kv7.5 homomeric channels that are inherently more sensitive to regulatory stimuli. Thus, our findings may advance our understanding of the roles Kv7.4 and Kv7.5 channels play in smooth muscle physiology and disease, particularly in conditions where Kv7.4 and Kv7.5 α-subunits are differentially expressed.

Molecular Pharmacology Fast Forward. Published on December 23, 2019 as DOI: 10.1124/mol.119.117192
This article has not been copyedited and formatted. The final version may differ from this version.

Authorship Contributions

Participated in research design: Brueggemann, Byron, and Cribbs
Conducted experiments: Brueggemann
Contributed new reagents or analytic tools: Cribbs
Performed data analysis: Brueggemann and Cribbs
Wrote or contributed to the writing of the manuscript: Byron, Brueggemann, and Cribbs

References

Boucherot A, Schreiber R and Kunzelmann K (2001) Regulation and properties of KCNQ1 (K(V)LQT1) and impact of the cystic fibrosis transmembrane conductance regulator. *J Membr Biol* 182: 39-47.

Brown DA and Passmore GM (2009) Neural KCNQ (Kv7) channels. *Br J Pharmacol* 156: 1185-1195.

Brueggemann LI, Cribbs LL, Schwartz J, Wang M, Kouta A and Byron KL (2018) Mechanisms of PKA-Dependent Potentiation of Kv7.5 Channel Activity in Human Airway Smooth Muscle Cells. *Int J Mol Sci* doi:10.3390/ijms19082223.

Brueggemann LI, Mackie AR, Cribbs LL, Freda J, Tripathi A, Majetschak M and Byron KL (2014) Differential Protein Kinase C-Dependent Modulation of Kv7.4 and Kv7.5 Subunits of Vascular Kv7 Channels. *J Biol Chem* 289: 2099-2111.

Brueggemann LI, Mackie AR, Mani BK, Cribbs LL and Byron KL (2009) Differential effects of selective cyclooxygenase-2 inhibitors on vascular smooth muscle ion channels may account for differences in cardiovascular risk profiles. *Mol Pharmacol* 76: 1053-1061.

Brueggemann LI, Mackie AR, Martin JL, Cribbs LL and Byron KL (2011) Diclofenac distinguishes among homomeric and heteromeric potassium channels composed of KCNQ4 and KCNQ5 subunits. *Mol Pharmacol* 79: 10-23.

Brueggemann LI, Moran CJ, Barakat JA, Yeh JZ, Cribbs LL and Byron KL (2007) Vasopressin stimulates action potential firing by protein kinase C-dependent inhibition of KCNQ5 in A7r5 rat aortic smooth muscle cells. *Am J Physiol Heart Circ Physiol* 292: H1352-H1363.

Byron KL and Brueggemann LI (2018) Kv7 potassium channels as signal transduction intermediates in the control of microvascular tone. *Microcirc* 25: e12419.

Byron KL and Taylor CW (1993) Spontaneous Ca^{2+} spiking in a vascular smooth muscle cell line is independent of the release of intracellular Ca^{2+} stores. *J Biol Chem* 268: 6945-6952.

Choveau FS, De la Rosa V, Bierbower SM, Hernandez CC and Shapiro MS (2018) Phosphatidylinositol 4,5-bisphosphate (PIP2) regulates KCNQ3 K(+) channels by interacting with four cytoplasmic channel domains. *J Biol Chem* 293: 19411-19428.

Delmas P and Brown DA (2005) Pathways modulating neural KCNQ/M (Kv7) potassium channels. *Nat Rev Neurosci* 6: 850-862.

Erdem FA, Salzer I, Heo S, Chen WQ, Jung G, Lubec G, Boehm S and Yang JW (2017) Updating In Vivo and In Vitro Phosphorylation and Methylation Sites of Voltage-Gated Kv7.2 Potassium Channels. *Proteomics* doi:10.1002/pmic.201700015.

Etxeberria A, Santana-Castro I, Regalado MP, Aivar P and Villarroel A (2004) Three mechanisms underlie KCNQ2/3 heteromeric potassium M-channel potentiation. *J Neurosci* 24: 9146-9152.

Gamper N and Shapiro MS (2007) Regulation of ion transport proteins by membrane phosphoinositides. *Nat Rev Neurosci* 8: 921-934.

Haick JM, Brueggemann LI, Cribbs LL, Denning MF, Schwartz J and Byron KL (2017) PKC-dependent regulation of Kv7.5 channels by the bronchoconstrictor histamine in human airway smooth muscle cells. *Am J Physiol Lung Cell Mol Physiol* 312: L822-l834.

Hoshi N, Zhang JS, Omaki M, Takeuchi T, Yokoyama S, Wanaverbecq N, Langeberg LK, Yoneda Y, Scott JD, Brown DA and Higashida H (2003) AKAP150 signaling complex promotes suppression of the M-current by muscarinic agonists. *Nat Neurosci* 6: 564-571.

Iwasaki H, Murata Y, Kim Y, Hossain MI, Worby CA, Dixon JE, McCormack T, Sasaki T and Okamura Y (2008) A voltage-sensing phosphatase, Ci-VSP, which shares sequence identity with PTEN, dephosphorylates phosphatidylinositol 4,5-bisphosphate. *Proc Natl Acad Sci USA* 105: 7970-7975.

Jespersen T, Grunnet M and Olesen S-P (2005) The KCNQ1 Potassium Channel: From Gene to Physiological Function. *Physiol* 20: 408-416.

Kimes BW and Brandt BL (1976) Characterization of two putative smooth muscle cell lines from rat thoracic aorta. *Exp Cell Res* 98: 349-366.

Kosenko A, Kang S, Smith IM, Greene DL, Langeberg LK, Scott JD and Hoshi N (2012) Coordinated signal integration at the M-type potassium channel upon muscarinic stimulation. *EMBO J* 31: 3147-3156.

Li Y, Gamper N, Hilgemann DW and Shapiro MS (2005) Regulation of Kv7 (KCNQ) K^+ channel open probability by phosphatidylinositol 4,5-bisphosphate. *J Neurosci* 25: 9825-9835.

Lopes CM, Remon JI, Matavel A, Sui JL, Keselman I, Medei E, Shen Y, Rosenhouse-Dantsker A, Rohacs T and Logothetis DE (2007) Protein kinase A modulates PLC-dependent regulation and PIP_2-sensitivity of K^+ channels. *Channels (Austin, Tex)* 1: 124-134.

Mackie AR and Byron KL (2008) Cardiovascular KCNQ (Kv7) Potassium Channels: Physiological Regulators and New Targets for Therapeutic Intervention. *Mol Pharmacol* 74: 1171-1179.

Mani BK, Robakowski C, Brueggemann LI, Cribbs LL, Tripathi A, Majetschak M and Byron KL (2016) Kv7.5 Potassium Channel Subunits Are the Primary Targets for PKA-Dependent Enhancement of Vascular Smooth Muscle Kv7 Currents. *Mol Pharmacol* 89: 323-334.

Marx SO, Kurokawa J, Reiken S, Motoike H, D'Armiento J, Marks AR and Kass RS (2002) Requirement of a macromolecular signaling complex for beta adrenergic receptor modulation of the KCNQ1-KCNE1 potassium channel. *Science* 295: 496-499.

McLaughlin S, Wang J, Gambhir A and Murray D (2002) PIP(2) and proteins: interactions, organization, and information flow. *Ann Rev Biophys Biomol Struct* 31: 151-175.

Raguimova ON, Smolin N, Bovo E, Bhayani S, Autry JM, Zima AV and Robia SL (2018) Redistribution of SERCA calcium pump conformers during intracellular calcium signaling. *J Biol Chem* 293: 10843-10856.

Salzer I, Erdem FA, Chen WQ, Heo S, Koenig X, Schicker KW, Kubista H, Lubec G, Boehm S and Yang JW (2017) Phosphorylation regulates the sensitivity of voltage-gated Kv7.2 channels towards phosphatidylinositol-4,5-bisphosphate. *J Physiol* 595: 759-776.

Schroeder BC, Kubisch C, Stein V and Jentsch TJ (1998) Moderate loss of function of cyclic-AMP-modulated KCNQ2/KCNQ3 K^+ channels causes epilepsy. *Nature* 396: 687-690.

Sedivy V, Joshi S, Ghaly Y, Mizera R, Zaloudikova M, Brennan S, Novotna J, Herget J and Gurney AM (2015) Role of Kv7 channels in responses of the pulmonary circulation to hypoxia. *Am J Physiol Lung Cell Mol Physiol* 308: L48-L57.

Stott JB, Povstyan OV, Carr G, Barrese V and Greenwood IA (2015) G-protein betagamma subunits are positive regulators of Kv7.4 and native vascular Kv7 channel activity. *Proc Natl Acad Sci U S A* 112: 6497-6502.

Suh BC and Hille B (2002) Recovery from muscarinic modulation of M current channels requires phosphatidylinositol 4,5-bisphosphate synthesis. *Neuron* 35: 507-520.

Suh BC and Hille B (2008) PIP_2 is a necessary cofactor for ion channel function: how and why? *Annu Rev Biophys* 37: 175-195.

Zaydman MA and Cui J (2014) PIP_2 regulation of KCNQ channels: biophysical and molecular mechanisms for lipid modulation of voltage-dependent gating. *Front Physiol* 5: 195.

Zhang H, Craciun LC, Mirshahi T, Rohacs T, Lopes CM, Jin T and Logothetis DE (2003) PIP_2 activates KCNQ channels, and its hydrolysis underlies receptor-mediated inhibition of M currents. *Neuron* 37: 963-975.

Zhang H, Liu Y, Xu J, Zhang F, Liang H, Du X and Zhang H (2013) Membrane microdomain determines the specificity of receptor-mediated modulation of Kv7/M potassium currents. *Neurosci* 254: 70-79.

Footnote

The project described was supported by Award Number I01BX007080 from the Biomedical Laboratory Research & Development Service of the VA Office of Research and Development.

Molecular Pharmacology Fast Forward. Published on December 23, 2019 as DOI: 10.1124/mol.119.117192
This article has not been copyedited and formatted. The final version may differ from this version.

Figure legends

Figure 1. **The amino-terminus of Kv7.5 is necessary for forskolin-induced increase in current amplitude of chimeric Kv7.4-Kv7.5 channels.** Panels i: schematics of wild-type Kv7.5 (A), wild-type Kv7.4 (B) and various Kv7.4- Kv7.5 chimeric constructs (D-G). Red lines indicate Kv7.5 sequence composition; blue lines indicate Kv7.4 sequence composition. Horizontal black lines indicate the membrane borders. Panels ii: Corresponding average (mean ± S.D.) normalized current-voltage (I-V) relationships before (closed circles) and during application of forskolin (1 μM for 15 min, open circles). Panels iii: Fractional conductance plots (mean ± S.D.) calculated from tail currents measured before (closed circles) and during application of forskolin (1 μM for 15 min., open circles), fitted to the Boltzmann distribution.

Figure 2. **Summary of forskolin-induced increase in current amplitude and effects on voltage-dependent activation of chimeric Kv7.4-Kv7.5 channels.** A. Summarized bar graph of forskolin (1 μM) -induced current enhancement through wild-type Kv7.5 (red), wild-type Kv7.4 (blue), and chimeric channels NKv7.5-Kv7.4, NKv7.5S53A-Kv7.4, NKv7.5-Kv7.4-ΔCKv7.5, NKv7.5-Kv7.4-CKv7.5, Kv7.4-CKv7.5, NKv7.4-Kv7.5, measured at -20 mV. * significant difference from all others ($P< 0.001$, One Way ANOVA). # significant difference from Kv7.4 ($P< 0.001$, One Way ANOVA). B. Voltage of half-maximal activation ($V_{0.5}$) of wild-type Kv7.5, wild-type Kv7.4, and chimeric channels abbreviated as in (A). * significant difference from Kv7.5 ($P< 0.001$, One Way ANOVA).

Figure 3. **Altered GPCR signaling responses of Kv7.4-Kv7.5 chimeric channels with amino- and carboxy-termini switched.** A-C. Average normalized current- voltage relationships of NKv7.5-Kv7.4 (A), Kv7.4-CKv7.5 (B) and NKv7.4-Kv7.5 (C) chimeric constructs before (close circles), during application of isoproterenol (1 μM for 10 min., open circles), and during application of AVP (100 pM, for 15 min, open circles). D-E. Summarized bar graphs of isoproterenol- induced current enhancement (D), and AVP-induced current inhibition (E), measured at -20 mV. *significant difference from Kv7.5 ($P< 0.001$, One Way ANOVA). # significant difference from all except Kv7.5 ($P< 0.001$, One Way ANOVA).

Figure 4. **Forskolin treatment preserves Kv7.5 channel function during Ci-VSP-induced PIP_2 depletion.** A. Representative traces of the Kv7.5 current recorded before (black) and after 10 min of forskolin (1 μM) application (red) in an A7r5 cell (C= 128 pF) co-expressing Kv7.5 and Ci-VSP. The voltage step protocol is depicted under the current traces. B. Time courses of forskolin-induced Kv7.5 current enhancement (filled circles) and of the rate of decline of current amplitude (open circles). Current enhancement was measured at -20 mV as the steady-state current during the last 500 ms of the voltage step, and normalized to average control current (n= 3). Rate of decline of current amplitude was calculated from the linear portion of the current recorded during each 10 s voltage step to +20 mV (n= 3). Arrow head indicates start of forskolin application. C. Summarized results of forskolin-induced Kv7.5 current enhancement (i) and forskolin-induced decrease of rate of decline of current Kv7.5 current amplitude (ii), based on last 5 min of control recordings and last 5 min of recordings in the presence of forskolin, averaged for each cell. * significant difference ($P< 0.05$, n=3, paired t-test). D. Averaged I-V curves normalized by the current measured at -20 mV before (black circles) and during application of forskolin (1 μM for 10 min, red circles, n=3). E. Summarized results of forskolin-induced effects on currents through NKv7.4-Kv7.5 channels (i) and forskolin-induced effects on rate of decline of NKv7.4-Kv7.5 current amplitude (ii). * significant difference ($P< 0.05$, n=4, paired t-test). F. Representative traces of the NKv7.4-Kv7.5 current recorded before (black) and after 10 min of forskolin (1 μM) application (red) in an A7r5 cell (C= 144 pF) co-expressing NKv7.4-Kv7.5 and Ci-VSP.

Figure 5. **Forskolin/IBMX treatment prevents decline of current amplitude of overexpressed or native Kv7.5 channels during Ci-VSP-induced or wortmannin-induced PIP_2 depletion.** A. Representative traces of exogenous wild-type human Kv7.5 current recorded in response to voltage steps (-80 mV, -20 mV and

Molecular Pharmacology Fast Forward. Published on December 23, 2019 as DOI: 10.1124/mol.119.117192
This article has not been copyedited and formatted. The final version may differ from this version.

+40 mV as indicated) before (control, black) and after 10 min treatment with forskolin (10 µM) and IBMX (500 µM) (red) in an A7r5 cell co-expressing Kv7.5 and Ci-VSP (C= 49.3 pF). B. Averaged I-V curves normalized by the current measured at -20 mV before (black circles) and during application of forskolin/IBMX (10 µM and 500 µM, respectively, for 10 min, red circles, n=5). * significant difference (P< 0.05, paired t-test). C. The time course of wortmannin-induced decline of native Kv7.5 current in A7r5 cells was measured at -20 mV and normalized by the average current measured before wortmannin application, following a pretreatment period of approximately 30 min with or without forskolin/IBMX (1 µM and 500 µM, respectively). Red and black traces represent means for forskolin/IBMX and non-pretreated groups, respectively. Light gray and dark gray traces are S.D. for black and red traces, respectively; n=4 for each group.

Figure 6. **Activation of PKC with PMA sensitized Kv7.5 channels to Ci-VSP-induced PIP_2 depletion.** A. Representative traces of the Kv7.5 current recorded in response to a double voltage step protocol and normalized by the current recorded at -20 mV before (black) and after 20 min treatment with 1 nM PMA (red) in an A7r5 cell co-expressing Kv7.5 and Ci-VSP (C= 121pF). The voltage step protocol is depicted under the current traces. B. Time courses of PMA-induced suppression of Kv7.5 current (filled circles) and of the rate of decline of current amplitude (open circles). Current enhancement was measured at -20 mV as the steady-state current during the last 500 ms of the voltage step, and normalized to average control current (n= 7). Rate of current decline was calculated from the linear portion of the current recorded during 10 s voltage step to 0 mV (n= 7). Arrow head indicates the start of PMA application. C. Summarized results of the extent of PMA- induced Kv7.5 current suppression (i) and PMA-induced increased rate of Kv7.5 current decline (ii); 5 min of control recordings and last 5 min of recordings in the presence of PMA were averaged for each cell. * significant difference (P< 0.05, paired t-test). D. Averaged I-V curves normalized by the current measured at -20 mV before (filled circles) and during application of PMA (1 nM for 20 min., open circles, n=7). * significant difference (P< 0.05, paired t-test).

Figure 7. **Time-dependent changes in membrane PIP_2 level upon treatment of A7r5 cells with forskolin/IBMX, PMA, and varying concentrations of AVP.** A. Time-course of average relative fluorescence intensity measured in A7r5 cells expressing PIP_2 sensor upon treatment with vehicle (0.1% DMSO, black, n= 15), PMA (1 nM, green, n= 13), forskolin/IBMX (10 µM forskolin (F) plus 500 µM IBMX, red, n= 11), carbachol in cells expressing M1 muscarinic receptor as positive control (50 µM Carb, blue, n= 7). B. Time-course of average relative fluorescence intensity measured in A7r5 cells expressing PIP_2 sensor upon treatment with AVP: 100 pM (blue, n= 12), 1 nM (green, n= 7), 10 nM (purple, n= 11). Arrow head indicate addition of the treatment. C. Change in fluorescence intensity measured as an average fluorescence in the last 30 s of the treatment relative to the average fluorescence in the last 30 s before treatment. * P< 0.05 relative to vehicle, One Way ANOVA on Ranks.

Figure 8. **Resting affinities for PIP_2 differ in Kv7.4 and Kv7.5 channels.** A. Averaged I-V curves normalized by the current measured at -20 mV in A7r5 cells co-expressing Ci-VSP with Kv7.5 (open circles, n=25) and Kv7.4 (filled circles, n=11). B. Time courses of averaged relative Kv7.5 current amplitudes measured at -20 mV and normalized by the amplitude at time 0 (current measured in response to the first voltage step applied 1 min after whole-cell formation) in the absence (open black circles, n=13) and in the presence of forskolin (10 µM) and IBMX (500 µM) (open red circles, n=9) fitted by an exponential decay function. Cell capacitances and access resistances ranged from 60 to 145 pF and 9 to 18 MΩ, respectively. C. Time courses of averaged relative Kv7.5 current amplitudes measured at -20 mV and normalized by the amplitude at time 0 (current measured in response to the first voltage step applied 1 min after whole-cell formation) in the absence (filled black circles, n=13) and in the presence of forskolin (10 µM) and IBMX (500 µM) (filled red circles, n=9) fitted by an exponential decay function. Cell capacitances and access resistances ranged from 59 to 190 pF and 7 to 15 MΩ, respectively, for Kv7.4 expressing cells.

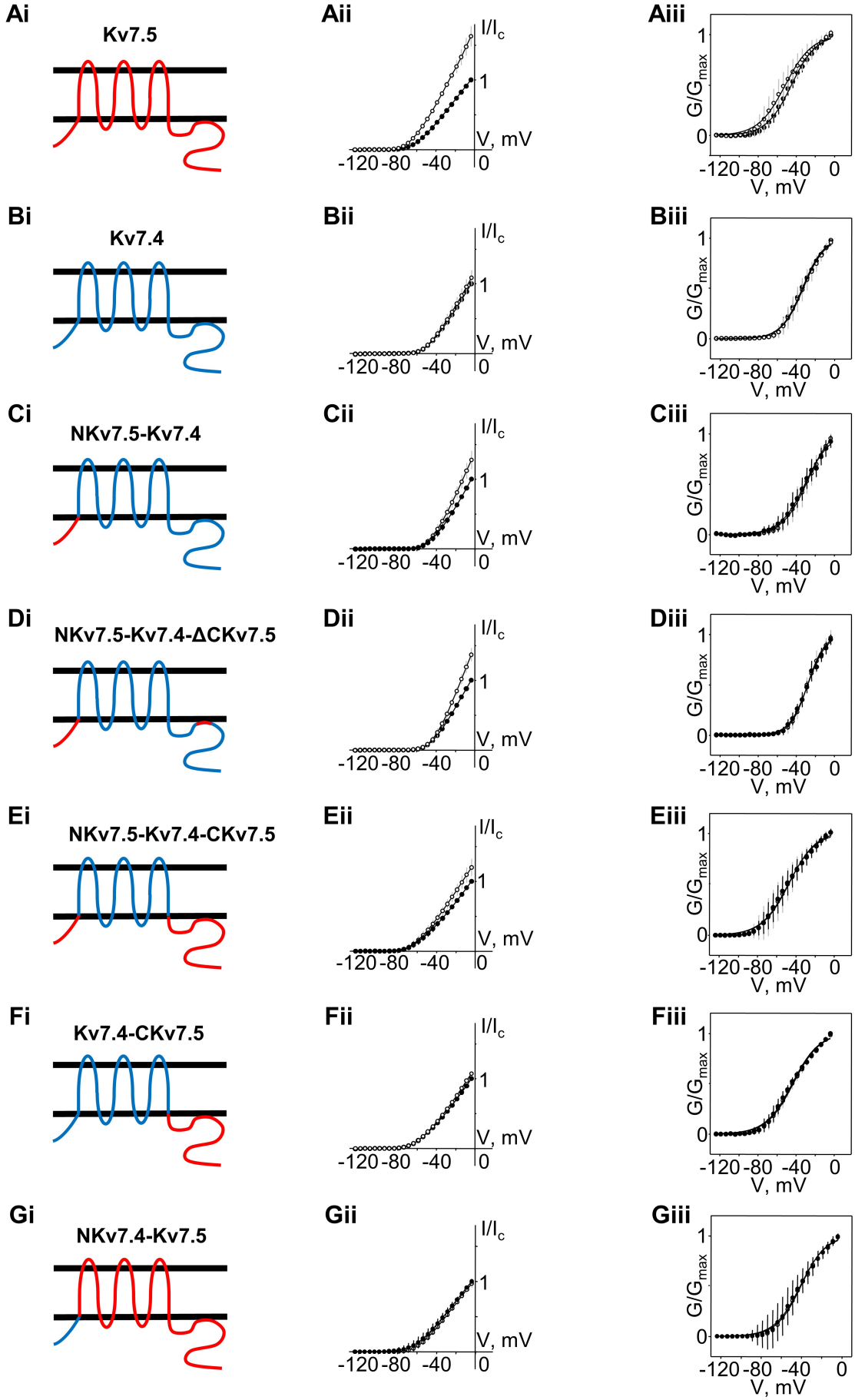
Ai
Kv7.5
Aii
I/Ic
1
V, mV
-120 -80 -40 0
Aiii
G/Gmax
1
0
-120 -80 -40 0
V, mV
Bi
Kv7.4
Bii
Biii
Ci
NKv7.5-Kv7.4
Cii
Ciii
Di
NKv7.5-Kv7.4-ΔCKv7.5
Dii
Diii
Ei
NKv7.5-Kv7.4-CKv7.5
Eii
Eiii
Fi
Kv7.4-CKv7.5
Fii
Fiii
Gi
NKv7.4-Kv7.5
Gii
Giii

Figure 1

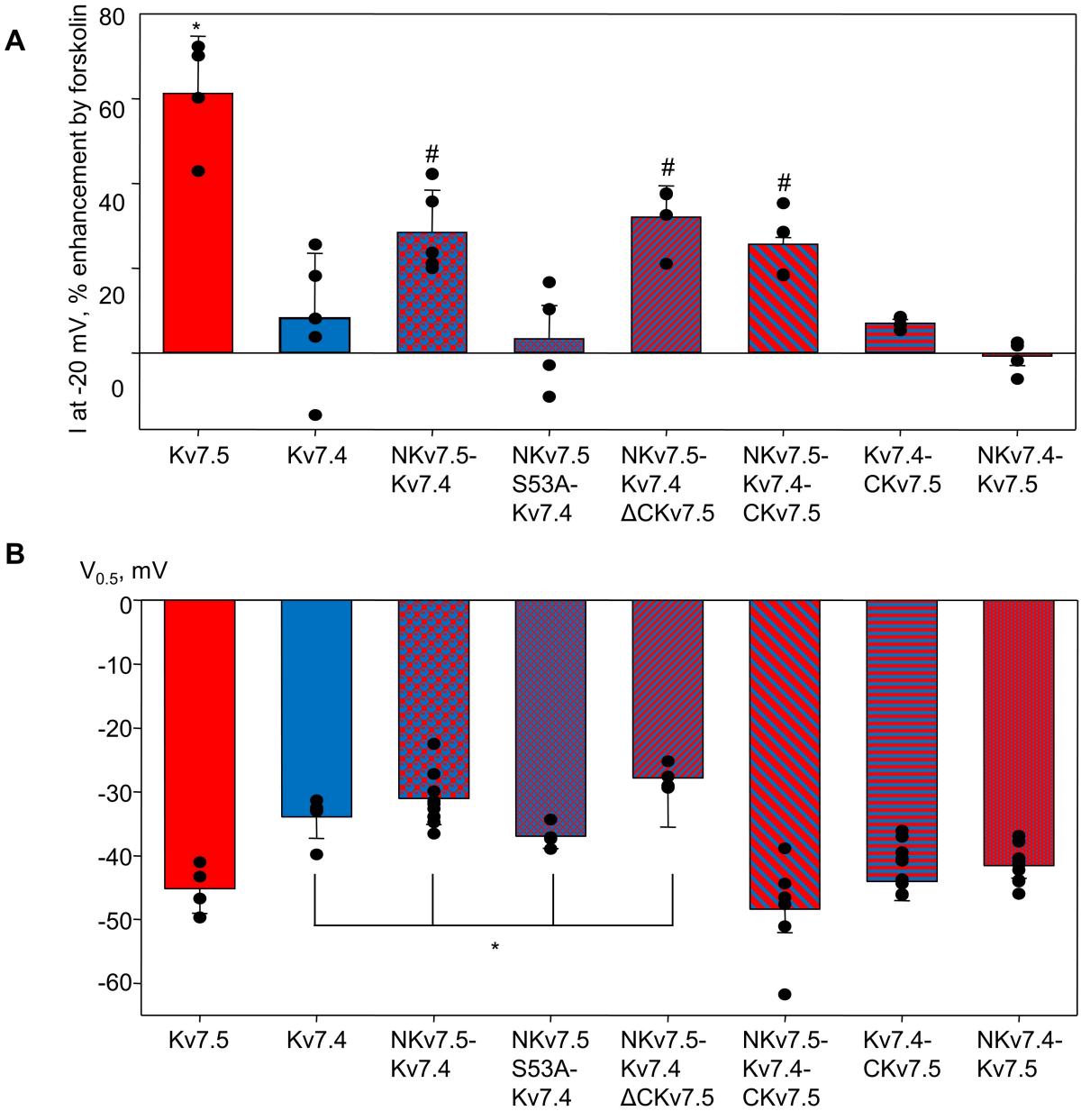
A
I at -20 mV, % enhancement by forskolin
80
60
40
20
0
*
#
#
#
Kv7.5
Kv7.4
NKv7.5-Kv7.4
NKv7.5 S53A-Kv7.4
NKv7.5-Kv7.4 ΔCKv7.5
NKv7.5-Kv7.4-CKv7.5
Kv7.4-CKv7.5
NKv7.4-Kv7.5
B
V0.5, mV
0
-10
-20
-30
-40
-50
-60
*
Kv7.5
Kv7.4
NKv7.5-Kv7.4
NKv7.5 S53A-Kv7.4
NKv7.5-Kv7.4 ΔCKv7.5
NKv7.5-Kv7.4-CKv7.5
Kv7.4-CKv7.5
NKv7.4-Kv7.5

Figure 2

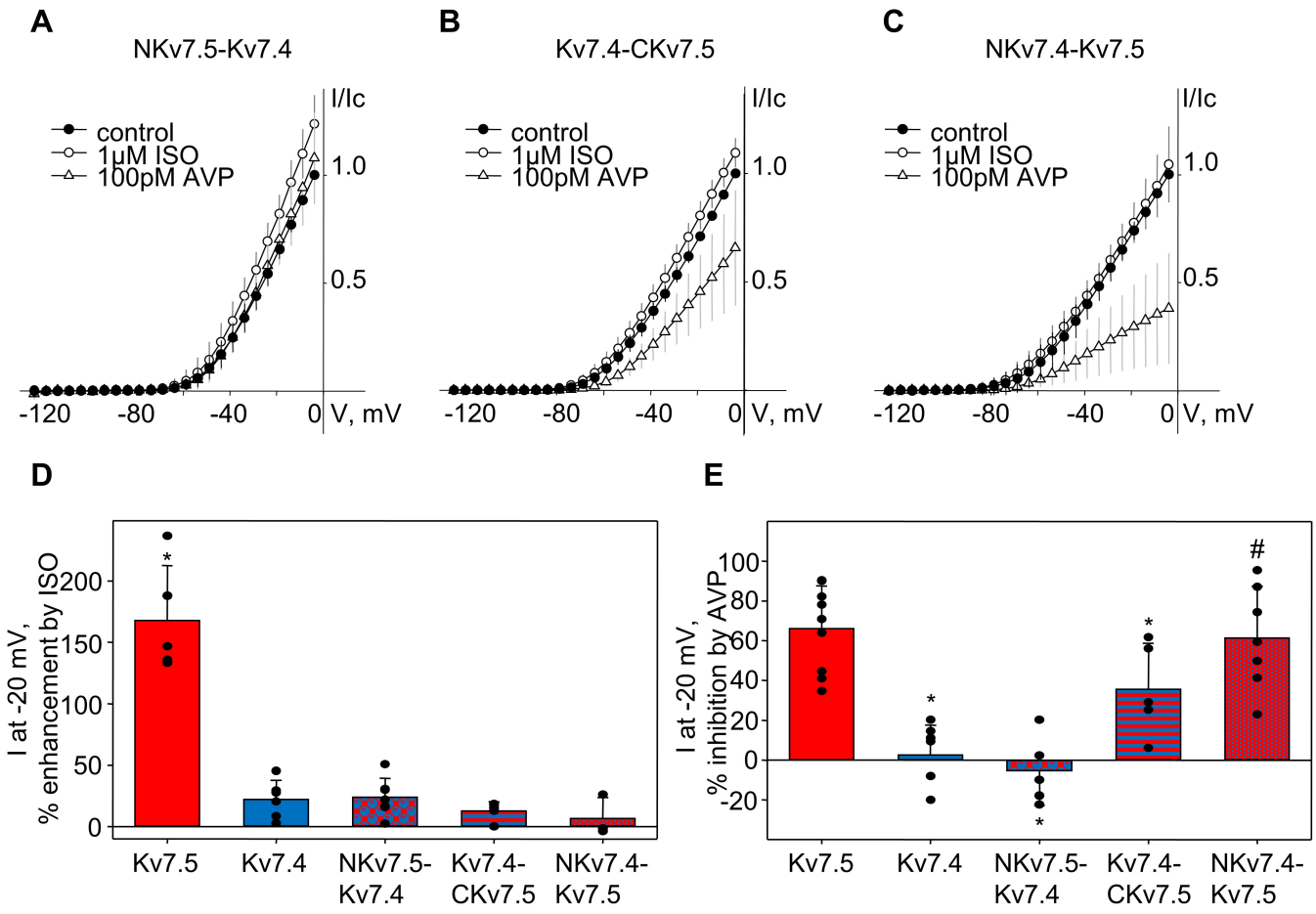
A
NKv7.5-Kv7.4
control
1μM ISO
100pM AVP
I/Ic
1.0
0.5
-120
-80
-40
0
V, mV
B
Kv7.4-CKv7.5
C
NKv7.4-Kv7.5
D
I at -20 mV,
% enhancement by ISO
200
150
100
50
0
Kv7.5
Kv7.4
NKv7.5-
Kv7.4
Kv7.4-
CKv7.5
NKv7.4-
Kv7.5
E
I at -20 mV,
% inhibition by AVP
100
80
60
40
20
0
-20
#

Figure 3

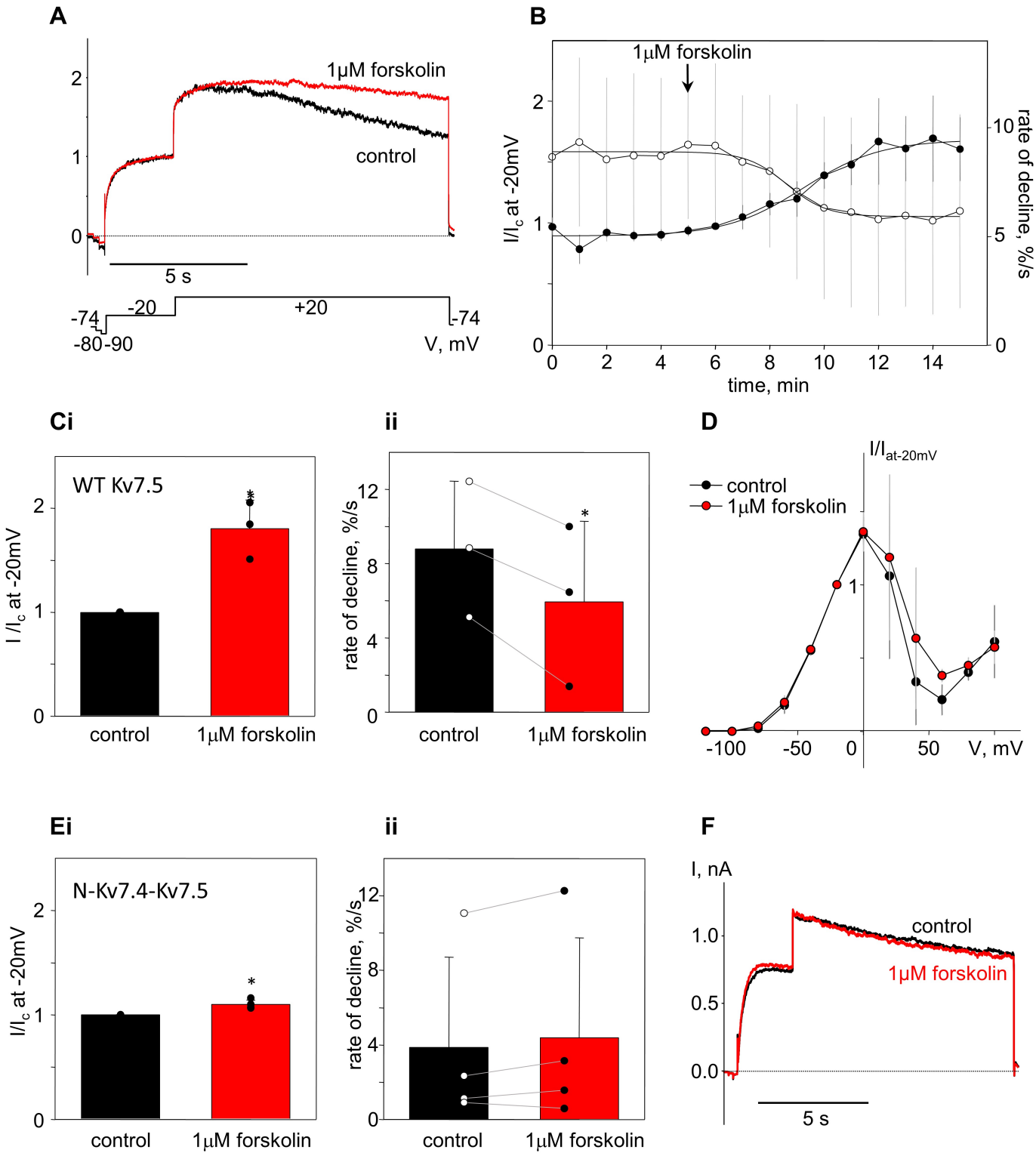
A
1μM forskolin
control
5 s
-74
-20
+20
-74
-80-90
V, mV
B
1μM forskolin
I/Ic at -20mV
rate of decline, %/s
time, min
Ci
WT Kv7.5
I /Ic at -20mV
control
1μM forskolin
ii
rate of decline, %/s
control
1μM forskolin
D
I/Iat-20mV
control
1μM forskolin
-100
-50
0
50
V, mV
Ei
N-Kv7.4-Kv7.5
I/Ic at -20mV
control
1μM forskolin
ii
rate of decline, %/s
control
1μM forskolin
F
I, nA
control
1μM forskolin
5 s

Figure 4

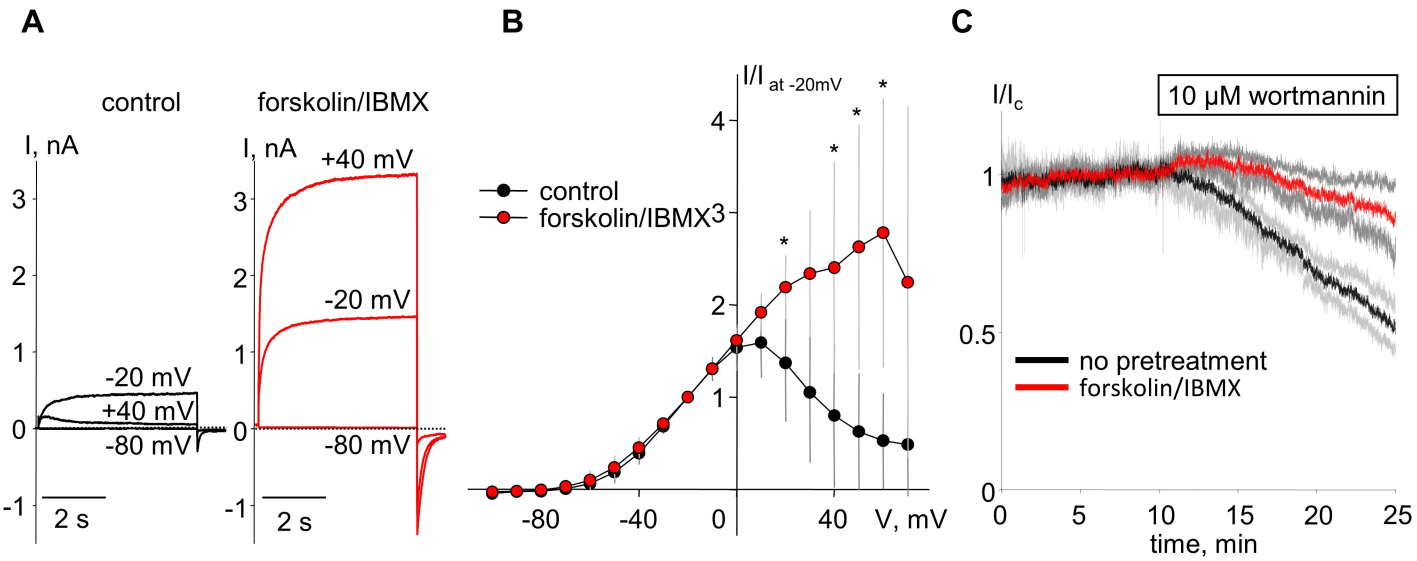
A
control
forskolin/IBMX
I, nA
-20 mV
+40 mV
-80 mV
2 s
B
I/I at -20mV
control
forskolin/IBMX
V, mV
C
I/Ic
10 µM wortmannin
no pretreatment
forskolin/IBMX
time, min

Figure 5

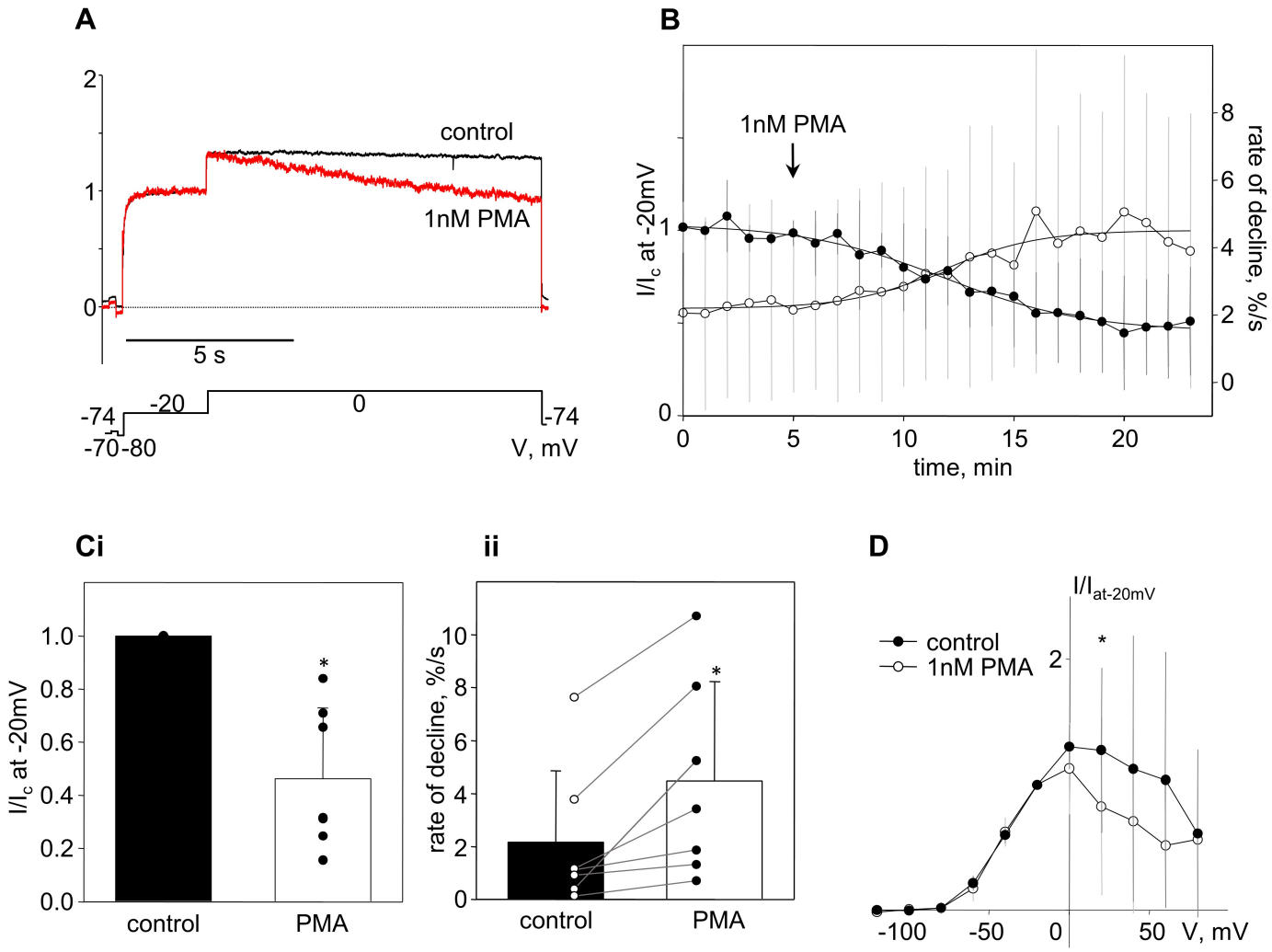
A
control
1nM PMA
5 s
-74
-20
0
-74
-70
-80
V, mV
B
1nM PMA
I/Ic at -20mV
rate of decline, %/s
time, min
Ci
ii
I/Ic at -20mV
rate of decline, %/s
control
PMA
control
PMA
D
I/Iat-20mV
control
1nM PMA
V, mV

Figure 6

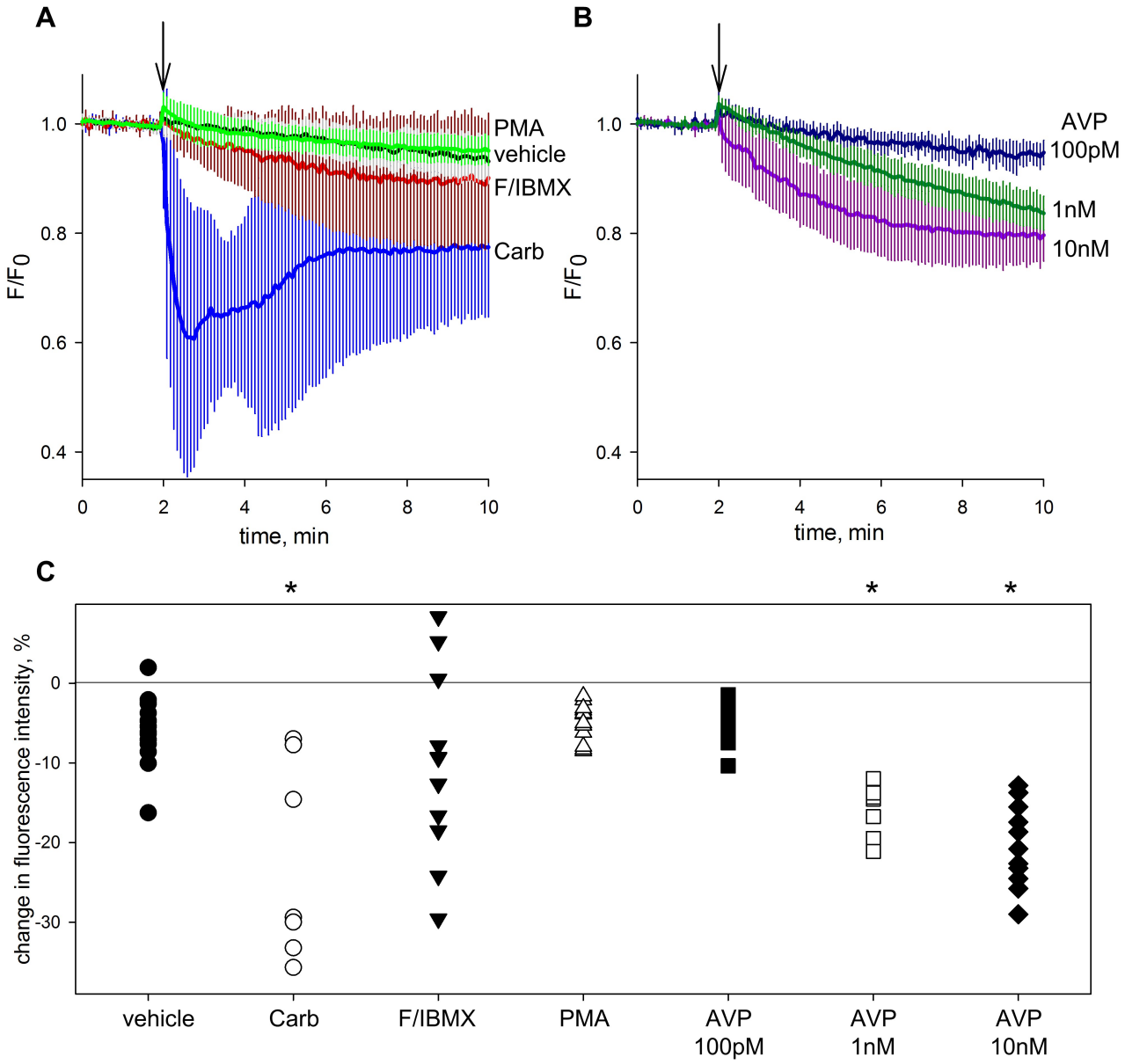
A
B
C
PMA
vehicle
F/IBMX
Carb
AVP
100pM
1nM
10nM
F/F0
time, min
change in fluorescence intensity, %
vehicle
Carb
F/IBMX
PMA
AVP
100pM
AVP
1nM
AVP
10nM

Figure 7

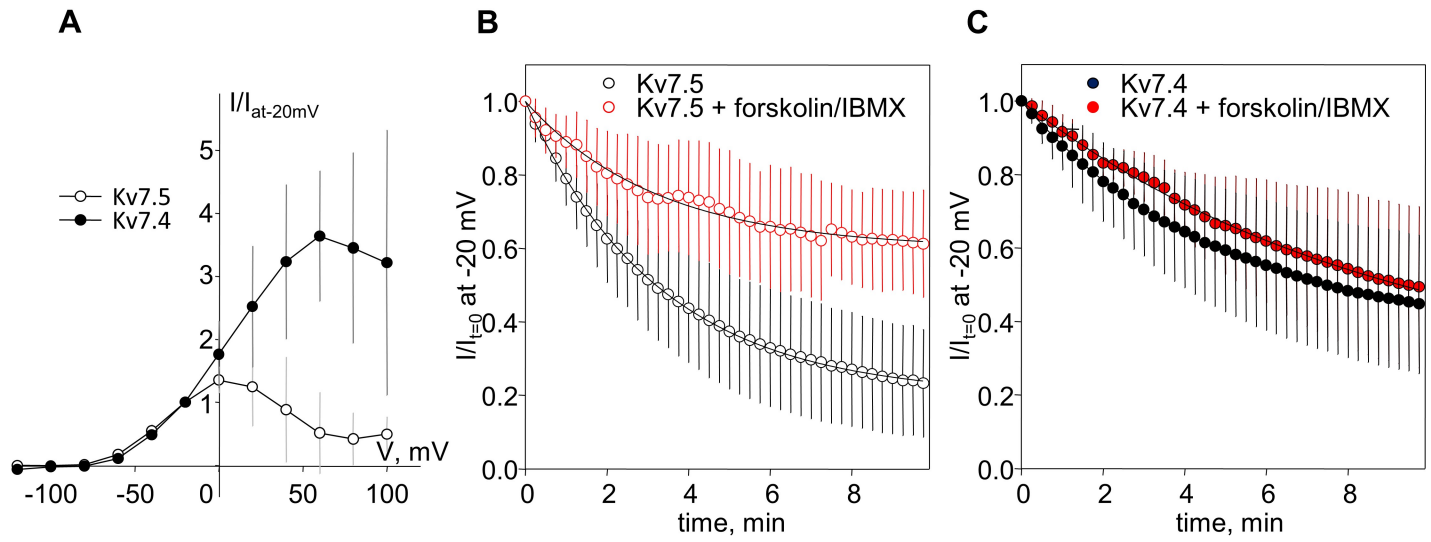
A
B
C
I/I at-20mV
Kv7.5
Kv7.4
V, mV
-100
-50
0
50
100
1
2
3
4
5
Kv7.5
Kv7.5 + forskolin/IBMX
I/I t=0 at -20 mV
time, min
0.0
0.2
0.4
0.6
0.8
1.0
0
2
4
6
8
Kv7.4
Kv7.4 + forskolin/IBMX

Figure 8